Development of Palm Kernel/Nanoparticles Surfactant and Study of Adsorption Behavior, Interfacial Tension Reduction and Wettability Alteration

Umar Hassan [a], Mohammed Falalu Hamza [a,b*], Hassan Soleimani [c], Sabiha Hanim Saleh[b], Saifullahi Shehu Imam[a] and Yarima Mudassir Hassan[d]
[a]*Department of Pure & Industrial Chemistry, Bayero University Kano, 3011 Kano, Nigeria*
[b]*School of Chemistry and Environment, Faculty of Applied Sciences, Universiti Teknologi MARA, 40450 Shah Alam, Selangor, Malaysia*
[c]*Department of Geosciences, Universiti Teknologi PETRONAS, 32610 Seri Iskandar, Perak Darul Ridzuan, Malaysia*
[d]*Department of Computer Science, Azman University Kano, 713140 Kano, Nigeria*

Abstract

Nanofluid is a promising technique for crude oil extraction in reservoirs by changing the interfacial tension (IFT) and wettability. This study aims to evaluate the capability of the nanofluid comprising palm kernel bio-surfactant (PS) and SiO_2 nanoparticles (NPs). The PS incorporated with the SiO_2 NPs revealed significant adsorption at various operation conditions. The optimal adsorption parameters of the palm kernel surfactant nanoparticles (PSNP) were found to be 120 minutes contact time, 0.2 %wt SiO_2 NPs dosage, 40 ^oC temperature, pH 9, and 3 % PS concentration. The adsorption isotherms data fitted with the Langmuir isotherm (R-squared value of 0.9). Furthermore, the nanofluid has demonstrated appreciable foam stability due to the good foam morphologies observed. It was found that PSNP nanofluid decreased the IFT of the oil/brine system from 6.22 mN/m to a low level of 1 x 10^{-2} mN/m. Additionally, the nanofluid changed the wettability to a 10% water-wet state. Consequently, PSNP biosurfactant foam can be utilized in foam flooding enhanced oil recovery (EOR) technique.

Keywords: *Enhanced oil recovery, Surfactant, nanoparticles, and adsorption.*

1. Introduction

Crude oil is a dominant primary source of energy and one of the developed marketplaces with the potential to address the global energy crisis [1-2]. On estimate, about 60-70 % of the oil remains in the reservoir after primary and secondary oil recovery methods are exhausted. The need for energy necessitates the application of diverse hydrocarbon recovery techniques including surfactant flooding [3]. Several factors affect oil extraction from the reservoirs such as wettability, interfacial tension (IFT) and negative capillary force [4]. A global increase in domestic and industrial demand for energy prompted the deployment of enhanced oil recovery (EOR) to lift up the potential oilfields [3]. Because of this demand, several hydrocarbon recovery techniques such as gas injection EOR, chemical EOR (surfactants, foams, polymers, alkaline solution and nanomaterials), thermal EOR and other EOR have

* Corresponding author. Tel.: +603-554-44534
E-mail address: hamzafalal84@gmail.com

Manuscript History:
Received 7 March 2025, Revised 11 April 2025, Accepted 14 April 2025, Published 30 April 2025

https://doi.org/10.33736/jaspe.9468.2025

e-ISSN: 2289-7771

been developed [4]. Surfactants play a vital role in many EOR systems, including surfactant flooding, foam flooding, and polymer flooding [5]. They have been considered revolutionary agents with exceptional EOR qualities due to their surface-acting capabilities, lowering oil-water IFT and modifying the rock's wettability [6]. The use of nanoparticles (NPs) in combination with surfactants to overcome the limitations of surfactant-based EOR techniques has gained unprecedented attention in recent years. This is mainly due to their nano size, thermal stability, and surface characteristics caused by the electrostatic interaction of the NPs with surfactant molecules [7]. Surfactants derived from plants are economically beneficial to oil industries due to their low toxicity, good biodegradability, and resource availability [8]. The kernel or inner seeds of oil palm fruits are the source of palm kernel oil (PKO), an edible plant oil that is used extensively in several industries, such as food and personal hygiene products. PKO is one of the few highly saturated vegetable fats that contain 16-carbon atoms of saturated fatty acid (palmitic acid) [9-10]. The main objective of this work is to create biosurfactant by utilizing Soxhlet extraction to extract the PKO. Subsequently, the biosurfactant is reinforced with SiO_2 NPs to generate nanofluid and study adsorption behavior via isotherm models. The optimum adsorption conditions are important to assess the foam foamability, stability, and morphology for EOR application.

2. Materials and methods

2.1. Determination of moisture

Mature palm kernel seeds were obtained from Rano Local Government Area (LGA), Kano State, Nigeria. The sample's initial and final masses were noted in each case before and after drying in the oven. The difference in mass relative to the final mass was expressed in percentage to determine the moisture content as given in (1).

$$Moisture\ content\ (\%) = \left\{\frac{Initial - final\ mass}{final\ mass}\right\} x100 \quad (1)$$

2.2. Determination of acid value

After precisely weighing 10.2 g of the sample, it was dissolved in a titration container and titrated potentiometrically with 0.1 N of potassium hydroxide solution (KOH) using (2).

$$\text{Acid value, mg}\frac{\text{KOH}}{\text{g}} = (A - B)\ x\ M\ x\ \left\{\frac{56.1}{W}\right\} \quad (2)$$

Where:
A = volume of KOH solution used in (ml),
B = volume for blank titration in (ml),
M = concentration of KOH in (mol/L),
W = sample, g.

2.3. Determination of Saponification value

Approximately, 2 g of the seeds powder sample were added to a mixture containing 25 ml of equal volumes of each ethanol and potassium hydroxide. The flask was assembled with a water bath

and attached to a reflux condenser of the Soxhlet apparatus. Thereafter, the mixture was heated for about 30 minutes at 60-70°C while being constantly stirred. After that, 1.0 ml of phenolphthalein indicator was added dropwise. A 0.5 N hydrochloric acid titration was performed on the resultant mixture. The same process was carried out again using a (blank) sample and (3) was used to determine the saponification value.

$$\text{Saponification value} = \left\{\frac{TD \; x \; N \; x \; 56.1}{M}\right\} \tag{3}$$

TD is the Titre difference (B-S) in ml, B represents the Titre blank in ml, and S is the Titre value in ml. The Normality (eq/L) of the titrating solution (KOH used herein) is described by N and M is the mass of the sample, (g).

2.4. Extraction & Synthesis

Precisely, 30 g of prepared Palm kernel (*Elaeis guineensis*) seeds were filled into the Soxhlet extractor. About 300 ml of ethanol was added to the mixture. The device was set up under distillation operation at a temperature of 60-65 °C below the boiling point of n-hexane. The extraction was repeated for about 9 times within three hours. For the synthesis, precisely 20 ml of the PKO was heated independently to between 80-90°C for 30 minutes to simmer the oils. 10 g NaOH was added by constantly stirring, and the mixture was heated at 80°C for roughly three hours. To find the functional groups, Fourier transform infrared (FTIR) spectroscopy was employed.

2.5. Adsorption studies

To determine the optimum concentration of the PS adsorbed onto the SiO_2 NPs, various concentrations of the PS (1, 2, 3, 4, and 5%wt) included a set quantity of 0.2%wt SiO_2 NPs which were made with 0.3%wt brine. After that, the mixtures were agitated for one hour at 300 rpm using an orbital shaker at 300 rpm for one hour while being monitored at a temperature of 37°C. All the filtrates were determined using a UV-spectrophotometer. The adsorption at equilibrium of the PS onto NPs was calculated (4). Other parameters, such as dosage, temperature, contact time and pH were also optimized.

$$\text{Adsorption (\%)} = \left\{\frac{Co-Ce}{W}\right\} \text{x } 100 \tag{4}$$

where Co is initial concentration of aqueous solution of surfactant (%wt), Ce is the final concentration of surfactant (%wt), and W is the weight of nanofluid (SiO_2) in (g).

2.6. Foam generation, stability & foam morphology

Ross-Mile's method was used to generate foams under turbulence force created when 5 ml of nanofluid passed through a standardized burette (75 x 1.5 cm) into the receiver vessel placed at 9.5 cm below the burette level. The maximum heights were measured and then allowed to collapse to observe the foam's half-lives ($t_{1/2}$) for 15 minutes. The average foamability and stabilities were noted, and the

experiments were conducted in duplicates. The foam bubbles were also studied under high-resolution microscopy to investigate the bubble sizes and their distribution.

2.7. IFT & contact angle analysis

The IFT analysis was carried out using an SVT20 spinning drop at 80^{o}C and 4000 rpm. First, the brine was added to the IFT tube, which was then put inside the chamber. After that, the tube was set under spinning at about 500 rpm, the rotation was able to keep the oil drop at the center of the tube. Subsequently, the rotation increased to about 4000 rpm stepwise to ensure drop stabilization. At this stage, the drop image was constantly captured by a camera attached to the equipment through which the IFT values were computed automatically using the principle of the Young Laplace equation. The contact angle was performed by a drop shape analyzer instrument. At first, slices of reservoir sandstones were submerged in different formulations of PSNP and one sample as a control (in brine). Thereafter, they were left for 48 hours to ensure adequate saturation and then contact angles were analyzed.

3. Results and discussion

3.1. Physico-chemical analysis

The physical and chemical properties of the oil and surfactant are given in Table 1. From the table, there is an indication of successful synthesis of surfactant due to significant functional groups identified. It can be seen that oil has a physical state of liquid at room temperature and the physical appearance (dark brown) is due to different chemical compositions [11]. Furthermore, the PKO seeds produced a content of oil yield (13%) while its saponification value assisted in determining the number of milligrams of KOH per gram of samples that could establish the synthesis of the surfactant. Moreover, oil has a higher saponification value which indicates suitability for surfactant synthesis. It can be established that the PKO having a high saponification value will have a lower acid average length [12]. This agrees with the acid number results obtained as the PKO contains fewer numbers of acid groups. The FITR spectra of PKO and PS are presented in Figure 1, and their respective frequencies are provided in Table 1. From the FTIR results, both indicate linear chains due to the presence of a peak at 729cm^{-1}, and the presence of -CH_2 and -CH_3 stretching vibrations noticed around 3000 cm^{-1}. The respective banding vibrations of -CH_2 and -CH_3 appeared around 1400-1200 cm^{-1}. The presence of ester -C=O and C-O were also noticeable.

Table 1. Physical properties and FTIR functional groups of Palm kernel oil (PKO) and its surfactant (PS) derivatives

Parameters	Oil properties	Func. Groups	Oil FTIR (cm^{-1})	PS FTIR (cm^{-1})
Nature of oil at room temp.	Liquid	-CH_2 and -CH_3 st*.	2921-2854	2921-2854
Colour of oil	Dark brown	-C=O st.	1746	Shift 1550
Yield of oil	13%	-CH_2 and -CH_3 bend.	1466-1235	1400-1300
Oil moisture (%)	6.02%	-C-O	1163	Shift 950
Saponification (mgKOH/g)	145.19	Long chain	729	729
Acid Number (mgKOH/g)	0.19	-	-	-
Mass of PS (g)	24.15	-	-	-

*St. is stretching.

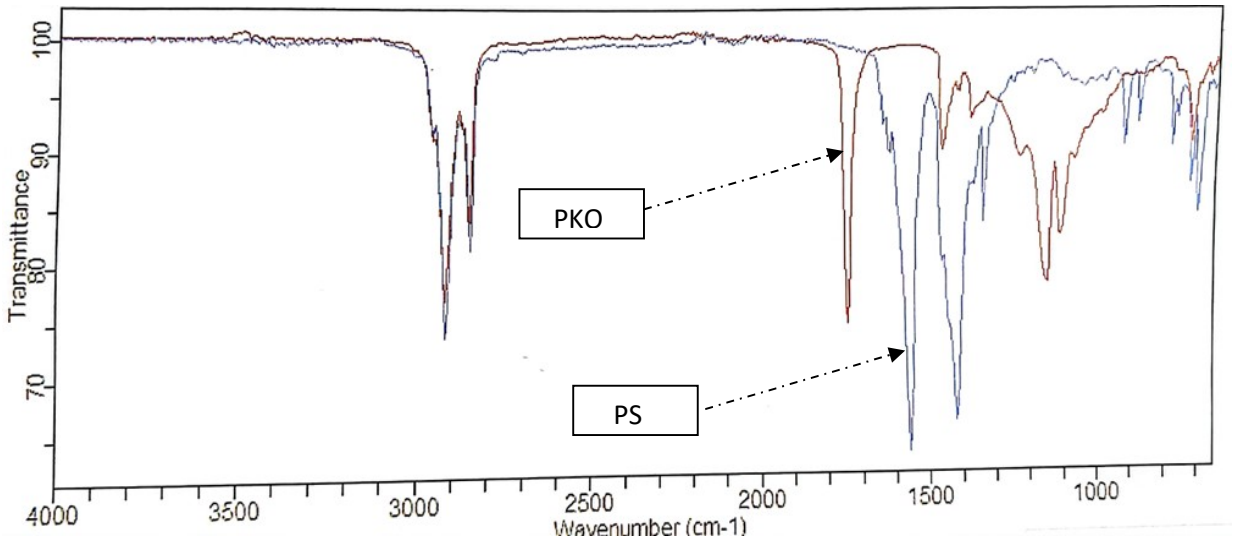

Figure 1. FTIR spectra of PKO and PS.

3.2. Adsorption studies

From the results in Figure 2a, the calibration plot of absorbance against concentration produced the R-squared value of 0.995. This data demonstrated a good correlation that can be used for subsequent adsorption studies. In Figure 2b, % adsorption of the PS was found to be 49.09% at 3%wt which indicates good efficiency of the PS in facilitating the adsorption onto NPs. This % adsorption demonstrates a strong affinity of interaction with the SiO_2 NPs. The higher % adsorption implies a greater surface coverage of the SiO_2 NPs [13]. The results of SiO_2 NPs dosage on % adsorption can also be observed in Figure 2c, and have shown a significant influence of the NPs dosage on adsorption, depicting interesting trends. It was observed that the maximum adsorption of 86 % was achieved at a dosage of 0.2 %. This dosage exhibited the highest affinity between PS and the SiO_2 NPs, leading to a substantial % adsorption [14]. From the result presented in Figure 2d, the PS exhibited a higher percentage of adsorption (61.1%) at 120 minutes. Economically, this suggests that the choice of surfactants and their interaction time significantly impact the adsorption process, and optimizing this parameter can enhance the overall efficiency of the PS and NPs interactions. Based on the data plot presented in Figure 2e, the effects of temperature on the adsorption of the PS onto SiO_2 NPs can be seen. It was observed that it exhibited a higher adsorption at 40 °C (54.7%). This result highlights the effect of temperature on the adsorption behavior of surfactants onto the NPs under constant operational conditions and optimized parameters such as dosage, contact time, concentration and others. Although the surfactants exhibited pH sensitivity behaviors, at pH 9 the % adsorption capacities were observed, i.e. the percentage adsorption of PS was found to be 61.64%. This is because the silica NPs often possess surface charges, and their electrostatic interactions with the surfactant molecules depend on the pH of the medium [15]. At specific pH values, the NPs surface charge may change, influencing the binding affinity of the surfactant molecules [13]. Also, surfactants may have ionizable groups, and their ionization state can be influenced by the pH of the medium. The degree of ionization affects the surfactant's hydrophilic and hydrophobic properties, determining how well it can interact with the NPs surface [16]. At certain pH levels, the attractive forces between the surfactant molecules and the nanoparticles may be minimized, and enhanced adsorption. Micelles can develop when the surfactant reaches its critical micelle concentration (CMC) at a specific pH. In order

to stabilize the colloidal suspension of the NPs and avoid agglomeration or precipitation, optimal adsorption at a particular pH is an important parameter [17].

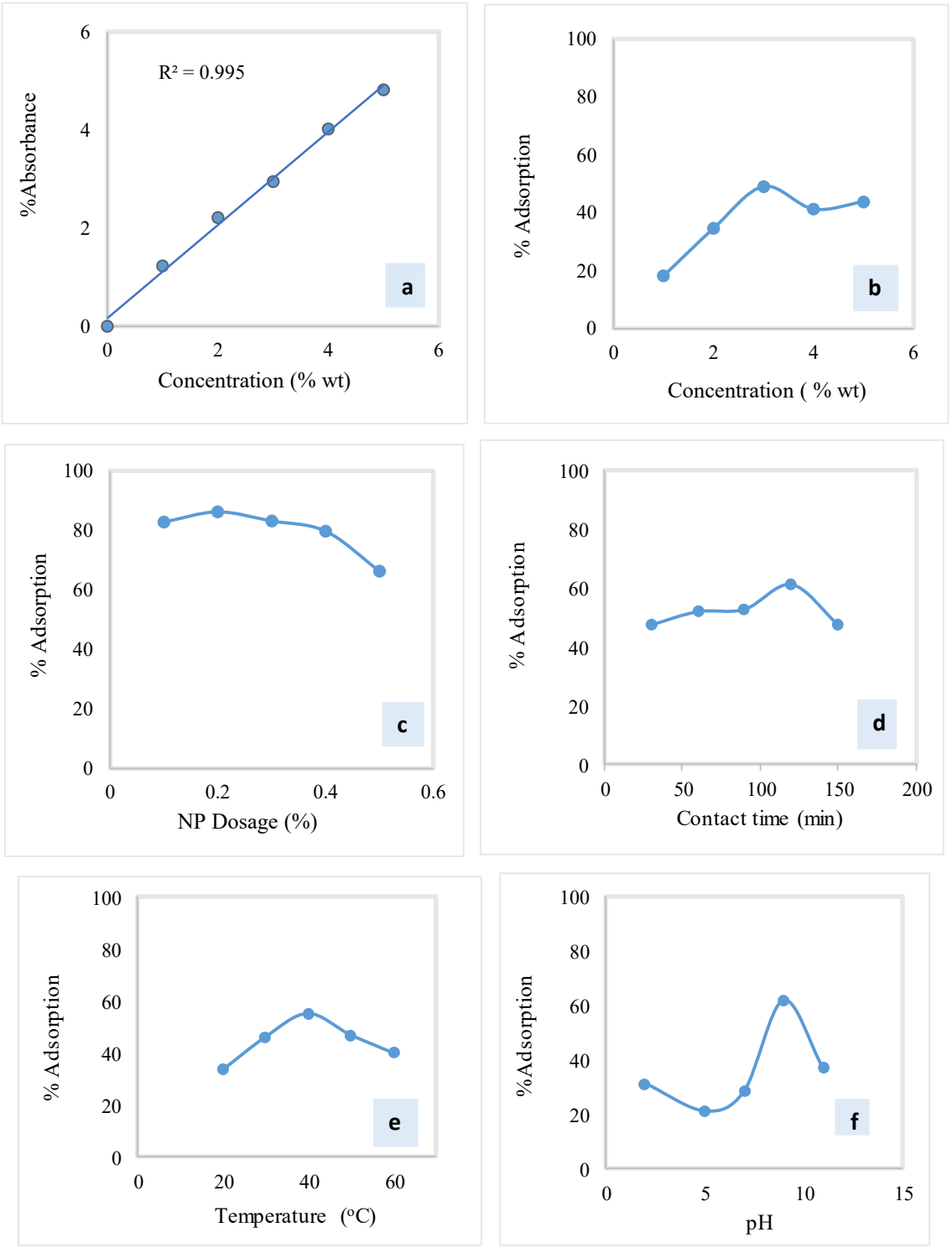

Figure 2. Results of (a) calibration curve to study the adsorption parameters (b) effect of PS concentration on a fixed amount of NPs to study % adsorption (c) effect of varying SiO_2 NPs dosage on % adsorption (d) effect of contact time between PS and NPs on % adsorption (e) effect of

increasing temperature on PSNP to study % adsorption; and (f) effect of pH from acidic to basic conditions on PSNP % adsorption.

Overall, the data from the adsorption isotherms show that the PSNPs experiment conformed better with the Langmuir isotherm because of a high R-squared value of 0.9417 (Figure 3a), rather than with the Freundlich's (Figure 3b). In Langmuir isotherm, the model presumes monolayer formation on the adsorbent surface having energetically equal homogeneous sites, with no lateral interaction and steric hindrance between the adsorbed molecules [18].

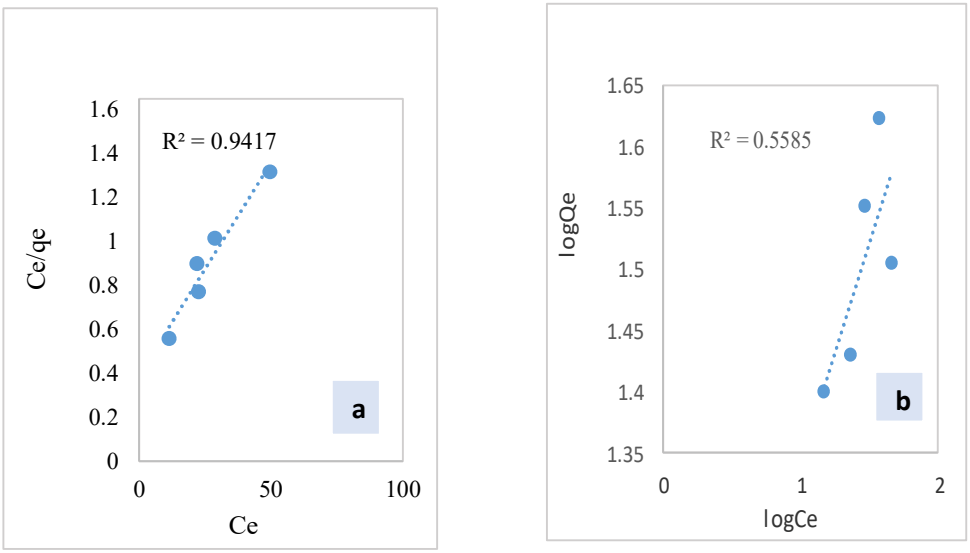

Figure 3. Plots of Langmuir (a) and Freundlich (b) isotherms for the study of adsorption of PS on NPs.

3.3. Results of foamability and stability

The foamability result is presented in Figure 4a. It was found that the initial foam heights for both PS and PSNPs were the same, signifying that the NPs did not influence the foamability of the PS. This could be related to the low concentration of the NPs used (0.2%) [19]. Contrary to the findings in this work, several studies have reported that the NPs could influence the foamability of various surfactants [20-22]. One of the important indicators of our observation is attributed to the nature of the PS surfactant molecules. It is pertinent that increasing the concentration could influence the foamability, but this study had taken cognizance of optimum adsorption dosage, thus higher concentration was anticipated to cause formation damage. However, as the time increased linearly, there was an overall height decrease for all the foams. Brine was observed to affect the initial foam heights, in agreement with many previously reported works [4, 23-24].

Furthermore, the foam $t_{1/2}$ is described as the time taken for the foam to decompose to half of its initial height (Figure 4b). The ratio of heights (t) to initial heights (t_o) was used to standardize the foam heights. The result indicates the direct relationship with foamability because the $t_{1/2}$ of the PS, PSNPs, and PSNPs+Brine, were found to be 4, 2, and 3.2 minutes, respectively. The quality and stability increased with the length of the $t_{1/2}$ [4].

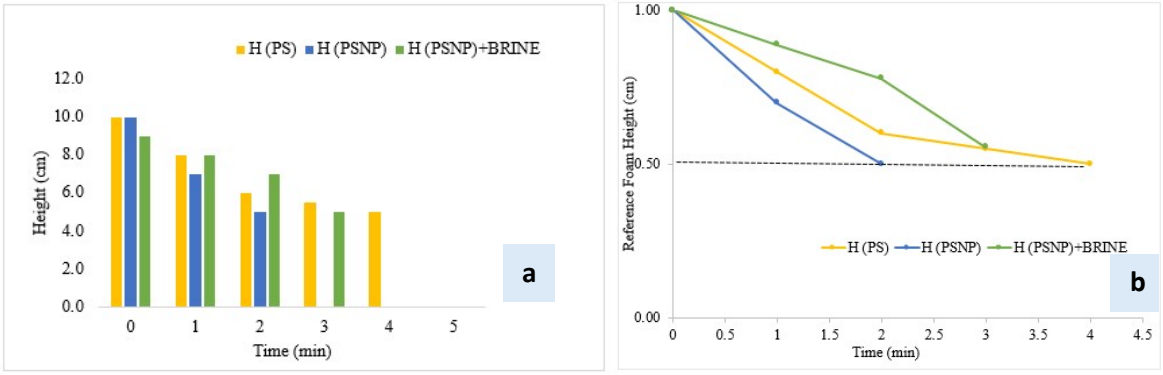

Figure 4. Plot (a) describes the average foam heights of formulations with time, and plot (b) presents the relative foam stabilities of formulations with time.

3.4. Foam morphology (Bubble size and distribution)

From the microscopic point of view, the foams were examined by measuring the sizes and counting the bubble number of bubbles per area. The average foam bubble sizes are presented in Table 2. The PS foams demonstrated that the bubble size increased linearly with time, indicating that as time increased, the size of bubbles increased considerably until they ruptured and collapsed due to coalescence. Upon addition of the NPs, it tended to decrease the bubble size which altered the rheology properties of the liquid phase in the foam, making additional resistance to drainage and coarsening of foam bubbles, preventing them from destabilizing.

Additionally, it was discovered that the presence of brine caused a linear increase in bubble size over time, which supported the effect of brine on foamability. There are three episodes of bubble coalescence, which include particle collision, rupture that results in a large bubble, and drainage of the liquid film.

Table 2. Change in foam bubble sizes and distributions with time generated from pure surfactant, surfactant with NPs and surfactant with NPs and brine

TIME (min)	PS Size(cm)	Bubble Distr. (cm)	PSNP Size(cm)	Bubble Distr. (cm)	PSNP+BRINE Size(cm)	Bubble Distr. (cm)
0.00	6.33	2.03-6.58	5.68	0.69-6.20	5.67	1.28-6.86
5.00	6.35	2.50-7.71	11.83	2.51-23.71	6.47	3.81-6.77
10.00	7.89	2.44-8.20	26.11	1.21-24.42	7.19	1.56-9.26

3.5. IFT & Contact angle Results

The initial IFT between the oil and the brine, which is regarded as a baseline, was described by the average IFT result of the oil-brine system, which was 6.22 mN/m, as indicated in Table 3. The average IFT values of the PS and PSNP significantly showed tremendous IFT reduction effects to ultralow levels of 4×10^{-3} and 1×10^{-2} mN/m, respectively. These additional decreases are ascribed to NPs and surfactant surface activity, respectively [1, 10].

The oil/brine system's first contact angle was determined to be approximately 20.58 ± 5° as shown in table 4. The maximum average contact angle is displayed by the control fluid. The control

fluid exhibits the highest average contact angle, suggesting a relatively less wetting surface. When the PS and the PSNP were analyzed in comparison with the control, there were significant reductions from 20.58 ± 5° of a baseline to 14.09 ± 2° for the PS and 18.47 ± 3° for the PSNP, respectively. This has demonstrated that the PS and the PSNP have abilities to alter the surface condition to preferred conditions due to wetting behaviors [21].

Table 3. The effects of brine, surfactant and NPs on IFT with increasing time

Time	Brine	PS	PSNP
20	6.2441	0.0032	0.0138
40	6.2445	0.0030	0.0140
60	6.3546	0.0042	0.0139
80	6.2440	0.0049	0.0143
100	6.0283	0.0049	0.0139
Average	6.22 ± 0.1	4×10^{-3}	1.3×10^{-2}

Table 4. The effects of brine, surfactant and NPs on the rock wettability

Parameters	Average (ca[o])	CA-Effect (CA[o])	Reduction (%)
BRINE	20.58 ± 5	-	-
PS	14.09 ± 2	6.49	32
PSNP	18.47 ± 3	2.11	10

4. Conclusion

From this study, there is a significant adsorption of the PS onto the NPs. Results show that the optimum percentage adsorption observed is at 120 min, 0.2%wt adsorbent and temperature of 40°C, pH9 and optimum concentration of 3%. These data fitted well with Langmuir isotherm having demonstrated R^2 of 0.9417. The nanofluid PSNP demonstrates a good IFT reduction and wettability property. This hybrid material is anticipated to have numerous uses in EOR.

Acknowledgements

The authors acknowledged Bayero University Kano, Nigeria, Universiti Teknologi MARA, Malaysia and Universiti Teknologi Petronas, Malaysia.

Conflict of interest

On behalf of all authors, the corresponding author states that there is no conflict of interest.

References

[1] Hamza, M.F., Sinnathambi C.M., Zulkifli, M. Aljunid Merican, Soleimani, H.,& Karl D. Stephen, (2018). Effect of SiO2 on the foamability, thermal stability and interfacial tension of a novel nano-fluid hybrid surfactant. *International Journal of Advanced and Applied Sciences,* 5(1), 113-122. https://doi.org/10.21833/ijaas.2018.01.015

[2] Hamza,M.F.,Hassan S.,H., Zulkifi, M.A., MSinnathambi,C.M.,Karl D.S., & Abdelazeem A.A. (2020). Nano-fluid viscosity screening and study of in situ foam pressure buildup at high-temperature high-pressure conditions. *Journal of Petroleum Exploration and Production Technology*, 10, 1115–1126 https://doi.org/10.1007/s13202-019-00753-

[3] Alireza, B. & Mojdeh Delshad. (2023). Strategy for Optimum Chemical Enhanced Oil Recovery Field Operation. *Journal Resource Recovery,* 1, 1001. https://doi.org/10.52547/jrr.2208.1001

[4] Hamza, M.F., Sinnathambi, C.M., & Merican, Z.M.A. (2017). Recent advancement of hybrid materials used in chemical enhanced oil recovery (CEOR): A review. *In IOP Conference Series: Materials Science and Engineering* 206(1), 012007. https://iopscience.iop.org/article/10.1088/1757-899X/206/1/012007/

[5] Al-Anssari, S., Ali, M., Alajmi, M., Akhondzadeh, H., Khaksar Manshad, A., Kalantariasl, A., & Keshavarz, A. (2021). Synergistic effect of nanoparticles and polymers on the rheological properties of injection fluids: implications for enhanced oil recovery. *Energy & Fuels*, 35(7), 6125-6135. https://doi.org/10.1021/acs.energyfuels.1c00105

[6] Kamal, M. S., Hussein, I. A., & Sultan, A. S. (2017). Review on surfactant flooding: phase behavior, retention, IFT, and field applications. *Energy & fuels*, 31(8), 7701-7720. https://doi/abs/10.1021/acs.energyfuels.7b00353

[7] Yekeen, N., Padmanabhan, E., Idris, A. K., & Ibad, S. M. (2019). Surfactant adsorption behaviors onto shale from Malaysian formations: Influence of silicon dioxide nanoparticles, surfactant type, temperature, salinity and shale lithology. *Journal of Petroleum Science and Engineering*, 179, 841-854. https://doi.org/10.1016/j.petrol.2019.05.041

[8] Muhammad, U. S., & Hamza, M. F. (2022). Fenugreek surfactant: Extraction, Synthesis and Evaluation of Foam Properties for Application in Enhanced Oil Recovery. *Applied Science and Technology Express*, 2022, 1-9. https://www.htpub.org/article/Applied-Science-And-Technology-Express/vol/2022/issue/0/articleid/1129

[9] Naksuk, A., Sabatini, D. A., & Tongcumpou, C. (2009). Microemulsion-based palm kernel oil extraction using mixed surfactant solutions. *Industrial Crops and Products,* 30(2), 194-198. https://doi.org/10.1016/j.indcrop.2009.03.008

[10] Davies, R. M. (2012). Physical and mechanical properties of palm fruit, kernel and nut. *Journal of Agricultural Technology*, 8(7), 2147-2156. http://www.ijat-aatsea.com

[11] Dollah, S., Abdulkarim, S.M, Ahmad, S.H., Khoramnia, A., Mohd, G.H. (2016). Physico-chemical properties of Moringa oleifera seed oil enzymatically interest with palm stearin and palm kernel oil and its potential application in food. *Journal Science Food Agric.* 96(10), 3321-3333. http://onlinelibrary.wiley.com/journal/10.1002/(ISSN)1097-0010

[12] Jekayinfa, S. O., & Bamgboye, A. I. (2007). Development of equations for estimating energy requirements in palm-kernel oil processing operations. *Journal of food engineering*, 79(1), 322-329. Doi:. 10.1016/j.jfoodeng.2006.01.045

[13] Liu, Z., Hedayati, P., Sudhölter, E. J., Haaring, R., Shaik, A. R., & Kumar, N. (2020). Adsorption behavior of anionic surfactants to silica surfaces in the presence of calcium ion and polystyrene sulfonate. *Colloids and Surfaces A: Physicochemical and Engineering Aspects,* 602, 125074. https://doi.org/10.1016/j.colsurfa.2020.125074

[14] Hashem, A., Aniagor, C. O., Farag, S., Fikry, M., Aly, A. A., & Amr, A. (2024). Evaluation of the adsorption capacity of surfactant-modified biomass in an aqueous acid blue 193 system. *Waste Management Bulletin*, 2(1), 172-183. https://doi.org/10.1016/j.wmb.2024.01.004

[15] Staniscia, F., Guzman, H. V., & Kanduč, M. (2022). Tuning contact angles of aqueous droplets on hydrophilic and hydrophobic surfaces by surfactants. *The Journal of Physical Chemistry B*, 126(17), 3374-3384. https://doi.org/10.1021/acs.jpcb.2c01599

[16] Rattanaudom, P., Shiau, B. J., Suriyapraphadilok, U., & Charoensaeng, A. (2021). Effect of pH on silica nanoparticle-stabilized foam for enhanced oil recovery using carboxylate-based extended surfactants. *Journal of Petroleum Science and Engineering*, 196, 107729. https://doi.org/10.1016/j.petrol.2020.107729

[17] Manyangadze, M., Chikuruwo, N. H. M., Chakra, C. S., Narsaiah, T. B., Radhakumari, M., & Danha, G. (2020). Enhancing adsorption capacity of nano-adsorbents via surface modification: A review. *South African Journal of Chemical Engineering*, 31(1), 25-32. https://doi.org/10.1021/acs.jpcb.2c01599

[18] Foo, K. Y., & Hameed, B. H. (2010). Insights into the modeling of adsorption isotherm systems. *Chemical engineering journal*, 156(1), 2-10. https://doi.org/10.1016/j.cej.2009.09.013

[19] Farhadi, H., Riahi, S., Ayatollahi, S., & Ahmadi, H. (2016). Experimental study of nanoparticle-surfactant-stabilized CO2 foam: Stability and mobility control. *Chemical Engineering Research and Design*, 111, 449-460. https://doi.org/10.1016/j.cherd.2016.05.024

[20] AlYousef, Z., Almobarky, M., & Schechter, D. (2017). Enhancing the stability of foam by the use of nanoparticles. *Energy & Fuels*, *31*(10), 10620-10627. https://doi.org/10.1021/acs.energyfuels.7b01697

[21] Rahman, A., Torabi, F., & Shirif, E. (2023). Surfactant and nanoparticle synergy: towards improved foam stability. *Petroleum*, 9(2), 255-264. https://doi.org/10.1016/j.petlm.2023.02.002

[22] Mohd, T. A. T., Shukor, M. A. A., Ghazali, N. A., Alias, N., Yahya, E., Azizi, A., ... & Ramlee, N. A. (2014). Relationship between foamability and nanoparticle concentration of carbon dioxide (CO2) foam for enhanced oil recovery (EOR). *Applied Mechanics and Materials*, 548, 67-71. https://doi.org/10.4028/www.scientific.net/AMM.548-549.67

[23] Youssif, M. I., Shoukry, A. E., Sharma, K. V., Goual, L., & Piri, M. (2024). The Effects of Brine Salinity and Surfactant Concentration on Foam Performance in Fractured Media. *Energy & Fuels*, 38(20), 19494-19508. https://doi.org/10.1021/acs.energyfuels.4c02706

[24] Rudyk, S., Al-Khamisi, S., & Al-Wahaibi, Y. (2021). Effects of water salinity on the foam dynamics for EOR application. *Journal of Petroleum Exploration and Production Technology*, 11(8), 3321-3332. https://doi.org/10.1007/s13202-021-01246-7